3D-QSAR Studies on Phthalimide Derivatives as HIV-1 Reverse Transcriptase Inhibitors

Weerasak Samee,[a] Jiraporn Ungwitayatorn,[b,*] Chutima Matayatsuk[b] and Jutarat Pimthon[b]

[a] Faculty of Pharmacy, Srinakharinwirot University, Nakhon Nayok, 26120, Thailand.
[b] Faculty of Pharmacy, Mahidol University, 447 Sri-Ayudhya, Bangkok 10400, Thailand.

* Corresponding author, E-mail: pyjuw@mahidol.ac.th

ABSTRACT: The novel non-nucleoside HIV-1 reverse transcriptase inhibitors in a phthalimide series were subjected to the three-dimensional quantitative structure-activity relationship (3D QSAR) studies using comparative molecular field analysis (CoMFA) and comparative molecular similarity indices analysis (CoMSIA). The best predictive CoMFA model gave cross-validated r^2 (q^2) = 0.688, non-cross-validated r^2 = 0.996, included the highest occupied molecular orbital (HOMO) energies in addition to CoMFA fields, and the best predictive CoMSIA model has q^2 = 0.629, non-cross-validated r^2 = 0.994, included steric, electrostatic, hydrophobic and hydrogen bond acceptor fields. A test set of 12 compounds was used to determine the predictive value of the models. The calculated (predicted) and experimental inhibitory activities were well correlated. The analysis of the 3D contour maps from both CoMFA and CoMSIA models offer important structural insight into designing novel and more active compounds prior to their synthesis.

Keywords: HIV-1 reverse transcriptase, phthalimide derivatives, Comparative molecular field analysis (CoMFA), Comparative Molecular Similarity Indices Analysis (CoMSIA).

INTRODUCTION

The virus-encoded reverse transcriptase (RT) plays an important role in the life cycle of the human immunodeficiency virus type 1 (HIV-1), the causative agent of AIDS. RT is an attractive target for the development of anti-HIV drugs for the treatment of AIDS. Several compounds targeted against HIV-1 RT have been shown to be active in clinical trials.[1-4] Nine drugs from two classes have been approved by the US FDA, namely, AZT, ddI, ddC, d4T, 3TC, abacavir, nevirapine, delavirdine, and efavirenz. The first six drugs are members of the nucleoside class and the others belong to the non-nucleoside class. The most recently approved RT inhibitor is tenofovir which belongs to nucleotide class.[5,6] Treatment by these drugs usually leads to the development of resistant HIV-1 mutants. The emergence of resistant strains has necessitated the continuation of research to find newer inhibitors. Recently, non-nucleoside HIV-1 RT inhibitors (NNRTIs) have played an important role in the treatment of HIV infections, and several of them have been investigated for use in alternative or combination therapy.[3,4] These compounds are highly active against HIV-1, but inactive against HIV-2 or any other retrovirus. This unique specificity of the NNRTIs for HIV-1 RT is due to the presence in HIV-1 RT, but not in other reverse transcriptases, of a flexible highly hydrophobic pocket.[7,8] The binding of the NNRTIs to the hydrophobic pocket of the HIV-1 RT does not interfere with the binding of the deoxynucleotide triphosphates (dNTPs), but slows down the rate of incorporation of the dNTPs in the DNA product.[9]

Previous investigations in our research group have identified the phthalimide derivatives as a new class of NNRTIs.[10] The synthesized compounds were tested *in vitro* for their HIV-1 reverse transcriptase inhibitory activity at concentration of 200 µg/mL by radiometric assay using polyadenylic acid (poly A) as template, oligodeoxythymidylic acid (oligo dT) as primer, and radiolabeled thymidine triphosphate ([³H]dTTP) as substrate. The activity was measured corresponding to the degree of inhibition of incorporation of [³H]dTTP into a polymer fraction by the synthesized compounds. The inhibitory activity was reported as percent inhibition as shown in Table 1. The most potent activity, IC_{50} = 60.90 µg/mL, was obtained with compound **22** (Table 2), whereas compounds **26** (Table 2), and **19** (Table 1) were less potent with IC_{50} = 98.10 µg/mL and 120.75 µg/mL, respectively.[10] These three compounds exhibited IC_{50} value lower than that of delavirdine (IC_{50} = 502.22 µg/mL, using poly rA.oligo dT as template-primer and [³H]dTTP as substrate) and AZT in HIV-1 strain M48, ddI-resistant strain (IC_{50} = 184.69 µg/mL, using poly rI.oligo dC as template-primer and [³H]dCTP as substrate).[11,12]

In this paper, two 3D QSAR methods, CoMFA and CoMSIA, were applied to investigate the correlations between *in vitro* HIV-1 reverse transcriptase inhibitory activity of the phthalimide derivatives and binding fields. The widely used CoMFA is based on the assumption that the interactions between a receptor and its ligands are primarily noncovalent in nature and shape-dependent.[13,14] Therefore, a QSAR may be derived from sampling the steric (Lennard-Jones) and electrostatic (Coulombic) fields surrounding a set of ligands and correlating the differences in those fields to biological activity. Partial least squares (PLS) analysis, with a cross validation procedure, was employed to select relevant components from the large set of CoMFA data to build up the best QSAR equation. The more recently reported CoMSIA approach calculated property fields based on similarity indices of drug molecules that have been brought into a common alignment.[15,16] The fields of different physicochemical properties used a Gaussian-type distance dependence, and no singularities occur at the atomic positions. The fields were evaluated by a PLS analysis similar to CoMFA. The results from these studies will be helpful to design new and more potent enzyme inhibitors.
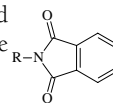
MATERIALS AND METHODS

A series of phthalimide derivatives listed in Tables 1 and 2 were tested for their HIV-1 RT inhibitory activity by a radiometric assay.[10,17-19] The results of the inhibitory activity were reported as percent inhibition and were used as dependent variables in this study. The test set compounds were selected based on the criteria that the percent inhibition of the test set should be in the range of percent inhibition of the training set and that the test set should be the representative of both active and inactive compounds.

Computational Details
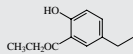*Generating the molecular structures and conformational analysis*

The molecular structures of phthalimide derivatives were modeled with SYBYL 6.8 molecular modeling program (Tripos Associates, Saint Louis, MO) on an Indigo Elan workstation (Silicon Graphics Inc., Mountain View, CA) using the sketch approach. The fragment libraries in SYBYL database were used as building blocks for the construction of larger ones. Each structure was first energy minimized using the standard Tripos force field (Powell method and 0.05 kcal/(mol.Å) energy gradient convergence criteria) and electrostatic charge was assigned by the Gasteiger-Hückel method. These conformations were used as starting conformations to perform docking by Flexidock option in SYBYL (20). The conformations

Table 1. Compounds in the training set and their *in vitro* reverse transcriptase inhibitory activities.

Compound No.	R	Inhibition(%)
1		43
2		37
3		22
4		3
5		29
6		21
7		14
8		8
9		43
10		11
11		24
12		3
13		26
14		6
15		20
16		52
17		16
18		32
19		84 (IC$_{50}$=120.75 μg/mL)
20		61
21		43

Table 2. Compounds in the test set and their *in vitro* reverse transcriptase inhibitory activities.

Compound No.	R	Inhibition(%)
22	HO / HO — CH$_2$CH$_3$ (ethyl-catechol)	43 (IC$_{50}$=60.90 µg/mL)
23	HO / CH$_3$CH$_2$O — CH$_2$CH$_3$	37
24	methylenedioxyphenyl–propyl	22
25	thiophene–propyl	3
26	furan–propyl	29 (IC$_{50}$=98.10 µg/mL)
27	pyridine–methyl	21
28	pyridine–ethyl	8
29	pyridine–ethyl	43
30	pyridine–propyl	11
31	pyridine–propyl	24
32	H$_3$C–pyridine–ethyl	3
33	morpholine–propyl	26

obtained from docking were further optimized by MOPAC 6.0 (PM3) and these conformations were used in the following 3D QSAR studies.

Structural Alignment

Since no x-ray crystallographic data of molecules in the training set were available, two different alignment methods, superimposition and field fit, were performed.

Superimposition

The superimposition of molecules was based on trying to minimize root-mean-squares (rms) differences in the fitting of selected atoms with those of a template molecule. Compound **19** with the highest percent inhibition (84%) was used as template molecule. All atoms of the benzene moiety of the phthalimide structural element and the pyrazine ring were selected for superimposition. Conformations which exhibited minimum of rms after superimposition procedure, were selected and stored in the database for the next step.

Field Fit

The field fit procedure was used as the second alignment criteria to increase field similarity within a series of molecules. In the field fit operation, the rms difference in the sum of steric and electrostatic interaction energies averaged across all (possibly weighted) lattice points between molecules in the training set molecule and template molecule was minimized to find the best fit. The same template molecule and atoms of template molecule were also used in field fit alignment. All molecular conformations obtained from superimposition were used to calculate the steric and electrostatic field around the molecules to find the best field fit.

CoMFA Set up

CoMFA was performed using the QSAR option of SYBYL version 6.8. The steric and electrostatic energies were generated using sp^3-carbon as probe atom with a +1 charge (default probe atom in SYBYL program). A 2.0 Å grid spacing and a distance-dependent dielectric constant were chosen. The cutoff value for both steric and electrostatic interaction was set to 30 kcal/mol at the beginning.

CoMSIA Set up

CoMSIA was performed using the QSAR option of SYBYL version 6.8. Five physicochemical properties (steric, electrostatic, hydrophobic, and hydrogen bond donor and acceptor) were evaluated, using a common probe atom with 1 Å radius, charge +1, hydrophobicity +1, hydrogen bond donor and acceptor properties +1. Similarity indices were calculated using Gaussian-type distance dependence between the probe and the atoms of the molecules of the data set. This functional form requires no arbitrary definition of cutoff limits, and the similarity indices can be calculated at all grid points inside and outside the molecule. The value of the attenuation factor a was set to 0.3.

PLS Calculations and Validations

PLS methodology was used for all 3D-QSAR analyses. The grid had a resolution of 2.0 Å and extended beyond the molecular dimensions by 4.0 Å in all directions. Column filtering was set to 2.0 kcal/mol. CoMFA and CoMSIA models were developed using the conventional stepwise procedure. The optimum number of components used to derive the non-validated model was defined as the number of components leading to the highest cross-validated r^2 (q^2) and the lowest standard error of prediction (SEP). The q^2 values were derived after "leave-one-out" cross-validation. The non-cross-validated models were assessed by the explained variance r^2, standard error of estimate (S) and F ratio. The non-cross-validated analyses were used to make predictions of the percent inhibitions of the phthalimide compounds from the test set and to display the coefficient contour maps. The actual versus predicted percent inhibitions of the test phthalimide compounds were fitted by linear regression, and the "predictive" r^2, S, and F ratio were determined.

QSAR Coefficient Contour Maps

The visualization of the results of the best CoMFA

Table 3. CoMFA results (grid space 2.0 Å, column filtering 2 kcal/mol and energy cutoff 40 kcal/mol).

Descriptors	Cross-validation			Non-crossvalidation		
	q^2	SEP	Optimal Components	r^2	S	F
steric+electrostatic+ HOMO	0.688	13.327	6	0.996	1.510	618.924

	Contributions		
	Steric	Electrostatic	HOMO
	0.343	0.476	0.181

and CoMSIA models have been performed using the "StDev*Coeff" mapping option contoured by contribution. Favored and disfavored levels fixed at 80% and 20%, respectively. The contours of the CoMFA and CoMSIA steric maps are shown in green (more bulk is favored) and yellow (less bulk is favored). The electrostatic fields of both CoMFA and CoMSIA contours are colored blue (positive charge is favored) and red (negative charge is favored). The contours of the CoMSIA hydrophobic fields are colored yellow (hydrophobic groups enhance activity) and white (hydrophilic groups enhance activity). The hydrogen bond field contours show regions where hydrogen bond acceptors (magenta) on the receptor enhance the activity and hydrogen bond donor (cyan) increase the activity.

RESULTS AND DISCUSSION

CoMFA Study

Schäfer et al.[21] described a pharmacophore model based on structural comparison and electronic properties of there NNRTIs, namely, TIBO, nevirapine and isoindolinone. Their pharmacophore consists of planes extended p-system and benzene ring arranged in a roof-like shape. This led us to use carbon atoms of the benzene moiety in the phthalimide nucleus and another aromatic ring (or alicyclic), which is pyrazine, of compound **19**, for molecular alignment. Superimposition and field fit were the two alignment criteria used in CoMFA study. The major objective when working with CoMFA is to find the best predictive model. Statistical results obtained from field fit alignment criteria gave better cross-validated r^2 (q^2) value than superimposition (data not shown) for every studied model. Therefore, only field fit alignment was used for further CoMFA studies. Column filtering values at 0.5, 1.0, 1.5 and 2.5 kcal/mol (which were different from the default setting at 2.0 kcal/mol), were investigated, but all led to a decrease in the q^2 value. Thus, the default setting column filtering 2.0 kcal/mol and energy cutoff 30 kcal/mol were used in the further studies. Several attempts have been made in order to improve the statistical outcomes such as varying grid space and energy cutoff, or including other physicochemical parameter (s), such as HOMO and LUMO energies. Table 3 summarizes the statistical results of the best obtained CoMFA model. Any field column with the deviation of less than 2.0 kcal/mol was excluded as well as any lattice point with the energy exceeding 40 kcal/mol was ignored from the PLS analysis. The best CoMFA model gave the $q^2 = 0.629$, $r^2 = 0.994$, $S = 1.90$, and $F = 389.280$, using steric and electrostatic fields and the HOMO energy. This CoMFA model was used to calculate the percent inhibition of all compounds in the training set. These results are compared to the experimental values in Table 4. Fig 1a shows the scattered plot of the predicted (calculated) and experimental percent inhibition of the training set. The test set (compounds **22**-**33**, Table 2), was used to evaluate the predictive ability of the CoMFA model. The predicted percent inhibition and the scattered plot of the test set are shown in Table 4 and Fig 1b, respectively.
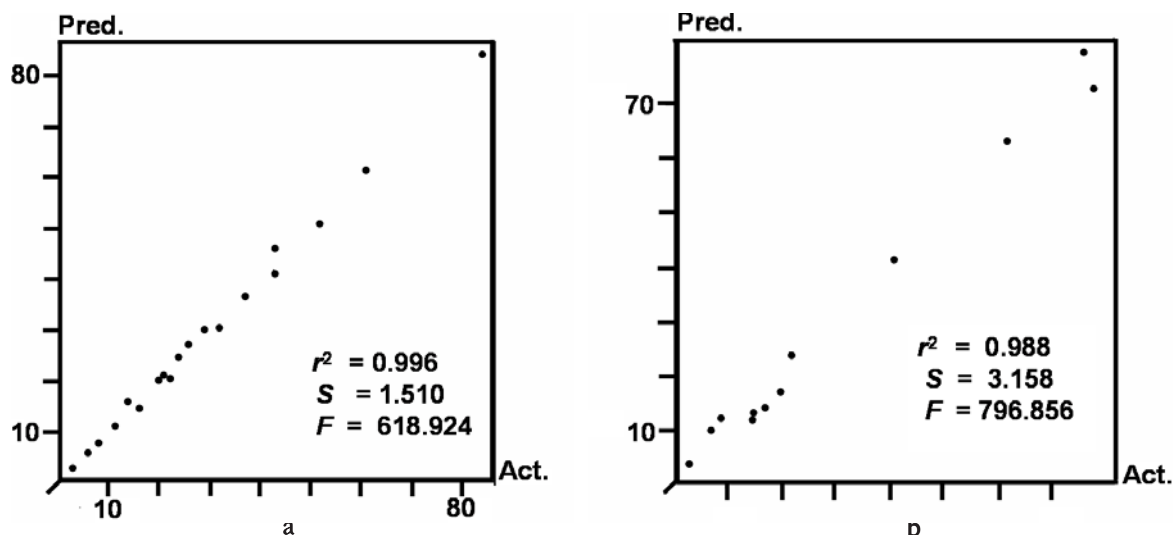
CoMSIA Study

The CoMSIA study was performed using the same PLS protocol and stepwise procedure as in the CoMFA analysis. By use of steric, electrostatic, hydrogen bonding, and hydrophobicity as descriptors, CoMSIA results are summarized in Table 5. The best CoMSIA model was found using 4 descriptor variables (steric, electrostatic, hydrogen bond acceptor and hydrophobic) with the $q^2 = 0.629$, $r^2 = 0.994$, $S = 1.90$, and $F = 389.280$. The hydrogen bond acceptor field explains 45.8% of the variance and the additional electrostatic field explains 23.5% of the variance. The summation of the CoMFA electrostatic (47.6%, Table 2) and HOMO energy (18.1%) is 65.7% which is approximately close to the summation of the CoMSIA hydrogen bond acceptor and electrostatic contributions (69.3%). Therefore, the electronic effect has more contribution to the inhibitory activity. The best CoMSIA model was used to predict the percent inhibition of the training set and the test set. The predicted and experimental percent inhibition and the scattered plots of both training set and test set are shown in Table 4 and Fig 2, respectively.

Table 4. Predicted activities vs. actual (experimental) activities and the residuals of CoMFA and CoMSIA.

Compound	Actual	CoMFA Predict	CoMFA Residuals	CoMSIA Predict	CoMSIA Residuals
Training set					
1	43	46.0	-3.0	40.2	2.8
2	37	36.6	0.4	36.6	0.4
3	22	20.4	1.6	22.9	-0.9
4	3	2.9	0.1	3.6	-0.6
5	29	30.2	-1.2	31.4	-2.4
6	21	21.2	-0.2	21.6	-0.6
7	14	15.9	-1.9	14.4	-0.4
8	8	8.1	-0.1	7.6	0.4
9	43	41.2	1.8	43.6	-0.6
10	11	11.2	-0.2	8.8	2.2
11	24	24.8	-0.8	24.9	-0.9
12	3	3.0	0.0	1.2	1.8
13	26	27.5	-1.5	25.6	0.4
14	6	6.1	-0.1	7.1	-1.1
15	20	20.3	-0.3	17.9	2.1
16	52	50.9	1.1	52.4	-0.4
17	16	14.6	1.4	17.2	-1.2
18	32	30.3	1.7	35.2	-3.2
19	84	84.1	-0.1	82.4	1.6
20	61	61.5	-0.5	62.3	-1.3
21	43	41.5	1.5	41.2	1.8
Test set					
22	76	67.7	8.3	68.0	8.0
23	22	23.6	-1.6	21.6	0.4
24	3	3.3	-0.3	3.4	-0.4
25	9	8.7	0.3	8.5	0.5
26	78	75.1	2.9	74	4.0
27	17	16.0	1.0	16.8	0.2
28	15	14.3	0.7	13.9	1.1
29	7	11.7	-4.7	5.7	1.3
30	20	19.7	0.3	17.7	2.3
31	15	16	-1.0	13.9	1.1
32	41	46.2	-5.2	42.5	-1.5
33	62	61.1	0.9	63.1	-1.1

The residuals of the predicted and experimental percent inhibitions of most of the compounds in the training set and test set were in the range of standard deviation derived from both CoMFA and CoMSIA QSAR models. As seen from Table 4, compound 22 shows the most outlier (giving residuals of 8.3 and 8.0, based on CoMFA and CoMSIA, respectively). This outlier can probably be attributed to the unusual hydrophilic character of compound 22 with 3,4-dihydroxy substitution on the phenyl ring since hydrophobic field contributes to the CoMSIA QSAR equation by 21.3 % (data as shown in Table 5).

The QSARs produced by CoMFA and CoMSIA models, which are usually represented as 3D "coefficient contour maps", are shown in Figure 3 and 4, respectively. The molecular structure of compound **19** was displayed inside the field as the reference structure. The steric and electrostatic contour maps from CoMFA and CoMSIA models indicate that bulky substituents should be located at position C-3 and methyl group of pyrazine and the positive charge substituents are preferred at position C-6 of the pyrazine nucleus. This structural requirement corresponds to the CoMSIA hydrophobic contour map (Fig 4c), which illustrates the hydrophobic region around position C-3 and methyl group of the pyrazine ring. The CoMSIA hydrogen bond acceptor contour map (Fig 4d) suggests that substituent at position 5 of the pyrazine should not be a hydrogen bond acceptor group and positions 1 and 4 should possess hydrogen bond acceptor group. In addition, this CoMSIA hydrogen bond acceptor contour map may also explain the high activity of compounds **22** and **26** (beside compound **19**) whose structures contain the hydrogen bond acceptor oxygen atom compared

Plot a (CoMFA training set):
r^2 = 0.996
S = 1.510
F = 618.924

Plot b (CoMFA test set):
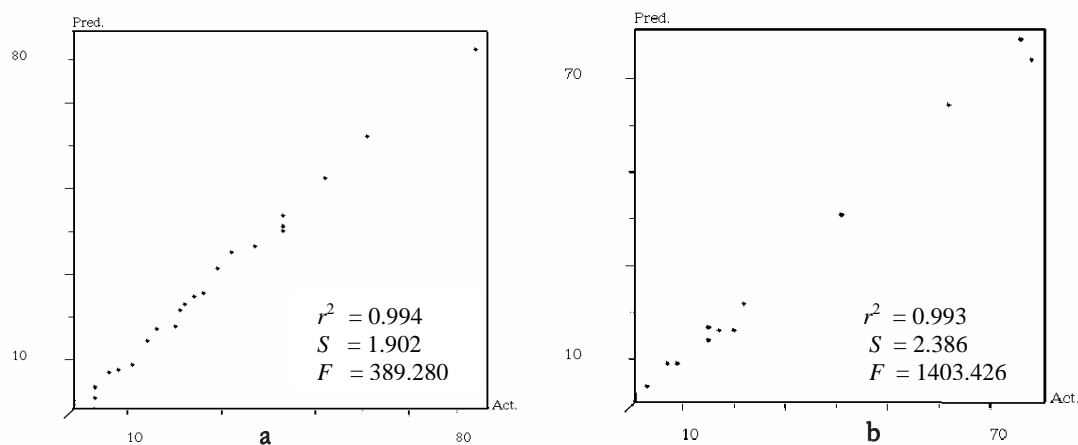r^2 = 0.988
S = 3.158
F = 796.856

Fig 1. Predicted vs actual percent inhibition for the training set (a) and the test set (b) obtained from CoMFA QSAR model.

Table 5. CoMSIA results.

Descriptors	Cross-validation		Non-crossvalidation		
	q^2	Optimal Components	r^2	S	F
Steric (S)	0.017	2	0.510	15.21	9.368
Electrostatic (E)	0.032	2	0.621	13.38	14.731
Electrostatic+steric	0.027	1	0.437	15.87	14.721
HB acceptor (A)	0.453	4	0.848	8.98	22.304
HB donor (D)	0.007	3	0.343	18.12	2.957
Acceptor + donor	0.433	6	0.860	9.23	14.289
Hydrophobic (H)	0.063	2	0.785	10.07	32.892
S+E+A+D+H	0.616	6	0.985	3.02	152.101
S+E+A+H	0.629	6	0.994	1.90	389.280

	Contributions		
Steric	Electrostatic	Hydrphobic	HB Acceptor
0.094	0.235	0.213	0.458

Fig 2. Predicted vs actual percent inhibition for the training set (a), and the test set (b) obtained from CoMSIA QSAR model.

$r^2 = 0.994$
$S = 1.902$
$F = 389.280$

$r^2 = 0.993$
$S = 2.386$
$F = 1403.426$
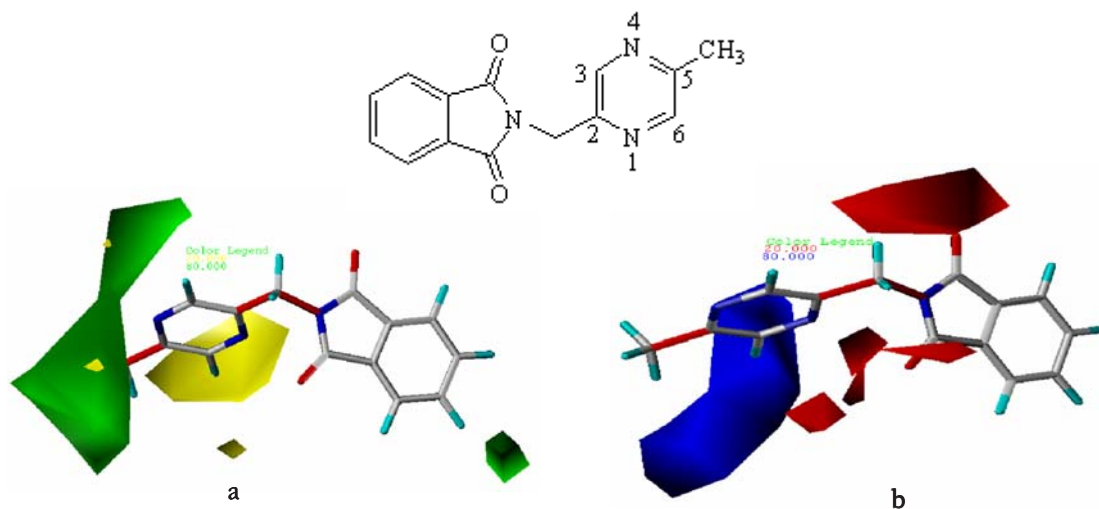
Fig 3. CoMFA contour maps: (a) Steric contour map: green and yellow polyhedra indicate regions where more steric bulk or less steric bulk, respectively, will enhance the activity. (b) Electrostatic contour map: blue and red polyhedra indicate regions where positively charged or negatively charged substituent will enhance the activity.
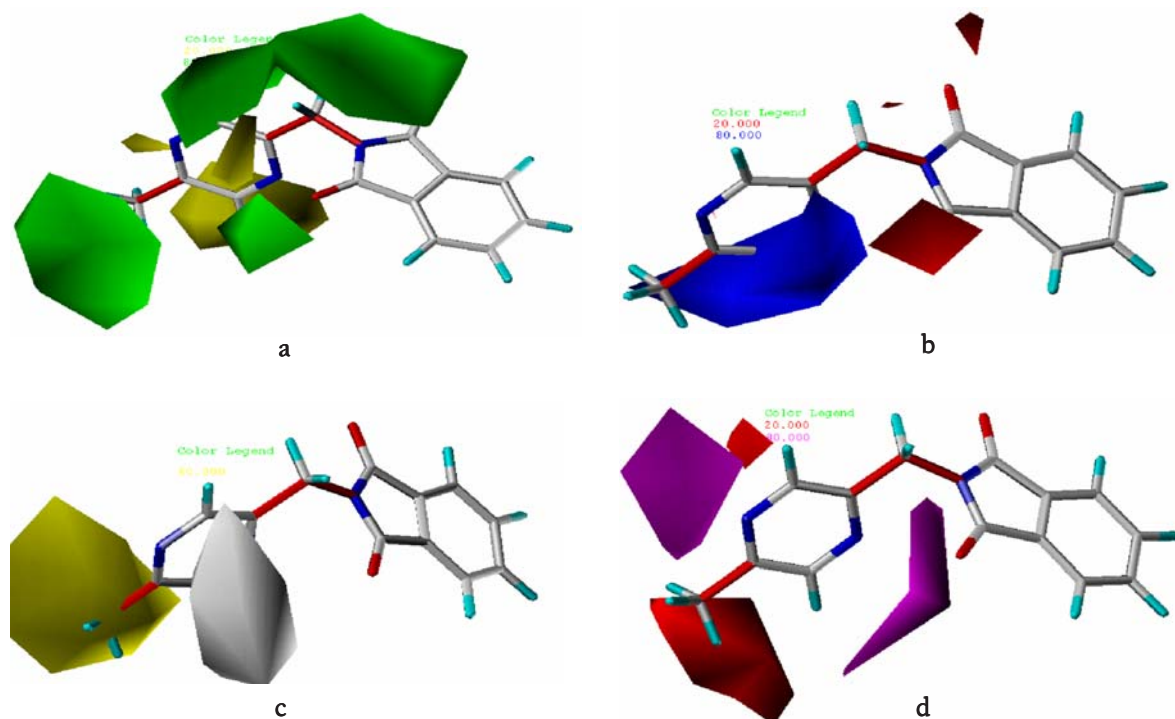
Fig 4. CoMSIA contour maps. (a) Steric contour maps. (b) Electrostatic contour maps. (c) Hydrophobic contour map: yellow and white polyhedra indicate regions where hydrophobic or hydrophilic groups, respectively, will enhance the activity. (d) Hydrogen bond acceptor ability contour map: magenta and red polyhedra indicate regions where hydrogen bond acceptor groups will increase or decrease the activity, respectively.   The colour codes for (a) and (b) are as described in Fig 3.

to compound 25 with lower hydrogen bond acceptor ability S atom. The CoMSIA contour map provides more details in the structural features required for the higher active compounds than CoMFA model alone.

In conclusion, the 3D QSAR using CoMFA and CoMSIA methods has been successfully applied to a set of recently synthesized phthalimide derivatives. The contour plots provide many useful insights into relationships between structural features and inhibitory activity and also give a picture of the main chemical features responsible for the good inhibitory activity. These features can be used to design new candidate compounds with higher activity.

ACKNOWLEDGEMENTS

REFERENCES

1. De Clercq E (1995) Antiviral therapy for human immunodeficiency virus infections. *Clin Microbiol Rev*, 200-239.
2. Mansour TS, Storer R (1997) Antiviral nucleosides. *Curr Pharm Des* **3**, 227-264.
3. De Clercq E (1999) Perspectives of non-nucleoside reverse transcriptase inhibitors (NNRTIs) in the therapy of HIV-1 infection. *IL Farmaco* **54**, 26-45.
4. De Clercq E (1999) The role of non-nucleoside reverse transcriptase inhibitors (NNRTIs) in the therapy of HIV-1 infection. *Antiviral Res* **38**, 153-179.
5. De Clercq E (2001) Antiviral drugs: current state of the art. *J Clin Virol* **22**, 73-89.
6. Fung HB, Stone EA, Piacenti FJ (2002) Tenofovir disoproxil fumarate: a nucleotide reverse transcriptase inhibitor for the treatment of HIV infection. *Clin Ther* **24**, 1515-1548.
7. Kohlstaedt LA, Wang J, Friedman JM, Rice PA, Steitz TA (1992) Crystal structure at 3.5 Å resolution of HIV-1 reverse transcriptase complexed with an inhibitor. *Science* **256**, 1783-90.
8. Nanni RG, Ding J, Jacobo MA, Hughes SH, Arnold E (1993) Review of HIV-1 reverse transcriptase three-dimensional structure: implications for drug design. *Perspect Drug Discovery Des* **1**, 129-50.
9. Spence RA, Kati WM Anderson KS, Johnson KA (1995) Mechanism of inhibition of HIV-1 reverse transcriptase by

non-nucleoside inhibitors. *Science* **267**, 988-93.

10. Ungwitayatorn J, Wiwat C, Matayatsuk C, Sripha K, Kamalanonth P (2001) Synthesis and evaluation of phthalimide and benzofuran derivatives as potential HIV-1 reverse transcriptase inhibitors. *Songklanakarin J Sci Technol* **23**(2), 235-45.

11. Genin MJ, Poel TJ, Yagi Y, Biles C, Athaus I, Keiser BJ, Kopta LA, Friis JM, et al (1996) Synthesis and bioactivity of novel bis (heteroaryl) piperazine (BHAP) reverse transcriptase inhibitors: Structure-activity relationships and increased metabolic stability of novel substituted pyridine analogues. *J Med Chem* **39**, 5267-75.

12. Schinazi, RF, McMillan, A, Cannon, D, Mathis R, Lloyd RM, Peck A, Sommadossi JP, St. Clair M, et al (1992) Selective inhibition of human immunodeficiency viruses by racemates and enantiomers of cis-fluoro-1-[2-(hydroxymethyl)-1,3-oxathiolan-5-yl] cytosine. *Antimicrob Agent and Chemothr* **36**(11), 2423-31.

13. Cramer III RD, Patterson DE, Bunce JD (1988) Comparative molecular field analysis (CoMFA). 1. Effect of shape on binding of steroids to carrier proteins. *J Am Chem Soc* **110**, 5959-67.

14. Cramer RD, Depriest SA, Patterson DE, Hecht P (1993) The developing practice of comparative molecular field analysis. In: Kubinyi H, editor. 3D QSAR in drug design: theory, method and applications, pp 443-85. ESCOM, Leiden.

15. Klebe G, Abraham U, Meitzner T (1994) Molecular similarity indices in a comparative analysis (CoMSIA) of drug molecules to correlate and predict their biological activity. *J Med Chem* **37**, 4310-46.

16. Klebe G, Abraham U (1999) Comparative molecular similarity index analysis (CoMSIA) to study hydrogen-bonding properties and to score combinatorial libraries. *J Comput-Aided Mol Design* **13**, 1-10.

17. Tan GT, Pezzuto JM, Kinghorn AD (1991) Evaluation of natural products as inhibitors of human immunodeficiency virus type 1 (HIV-1) reverse transcriptase. *J Nat Prod* **54**(1), 143-54.

18. Hoffman AD, Banapour B, Levy JA (1985) Characterization of the AIDS-associated retrovirus reverse transcriptase and optimal conditions for its detection in virions. *Virology* **147**, 326-35.

19. Kusumoto IT, Shimada I, Kakiuchi N, Hattori M, Namba T (1992) Inhibitory effects of Indonesian plant extracts on reverse transcriptase of an RAN tumour virus (I). *Phytother Res* **6**, 241-44.

20. Ungwitayatorn J, Sothipatcharasai P (2000) Docking Study on phthalimide derivatives: HIV-1 reverse transcriptase inhibitors. *Srinakharinwirot J Pharm Sci* **5**(1), 19-27.

21. Schäfer W, Friedbe WG, Leinert H, Mertens A, Poll T, von der Saal W, Zilch H, Nuber B, et al (1993) Non-nucleoside inhibitors of HIV-1 reverse transcriptase: molecular modeling and X-ray structure investigations. *J Med Chem* **36**, 726-32.